Flight Dynamics and Advanced Control

Coursework – TB1 2025

Ethan Sheehan
Student number: 2400720
Username: fc23871

Academic integrity statement: Google's Gemini-3 was used during code debugging in the form of error message explanations, also was used as a dictionary to search for MATLAB functions. No AI was used for data analysis or figure generation. AI was employed to give suggestion on how to condense text. The author has considered and included several suggested references and is fully accountable for the submitted work.

A1.1: Equations of Motion & Trim

A. Trimming and Linearization

For an aircraft to be successfully trimmed, all the forces and moments acting on the rigid body need to sum to 0 so that the aircraft is in a steady equilibrium state. Specific control inputs and state variables must be found to allows the aircraft maintain steady flight without without needing any pilot control input. [1]

The full rigid body dynamics are described by the non-linear vector function:

$$\dot{\mathbf{x}} = f(\mathbf{x}, \mathbf{u})$$

Achieving a trimmed state requires solving the nonlinear equations of motion to determine the state variable and control vectors necessary so that the time derivatives of the state variables are set to 0. This means there is no rate of change in the state variables, hence it will be trimmed [2]:

$$\dot{\mathbf{x}} = f(\mathbf{x_0}, \mathbf{u_0}) = 0$$

Linearization is the process of approximating the full nonlinear equations of motion of an aircraft to linear equations about a specific trimmed equilibrium state, assuming all pertubation in the trim condition are small. This allows for high-order terms or terms involding the products of small quantities to be neglected resulting in a set of linear-time-invariant differential equations. These LTI equations relate small perturbations in motion or control inputs to accelerations of the aicraft. Linearization enables the use of eigenvalue analsys, state space mathods, transfer functions, and other tools to more easily evaluate the nonlinear system. [3]

B. Longitudinal trim and Lateral-Directional trim

The longitudinal trim condition (steady level flight) is when the aircraft maintains constant velocity and altitude with wings level and zero sideslip. The longitudinal trim condition requires the elevator angle and thrust to be adjusted simultaneously to provide a longitudinal equlibrium flight state at a given airspeed and flight path angle. [4]

In order to numerically solve for this trim condition, the non-linear equations for axial force, normal force, and pitching moment must be solved. These equations are coupled due to a change in elevator angle affecting the overall lift and drag of the aircraft, changing the required thrust and angle of attack required to stay level. The axial force equation balances the thrust against drag and the component of weight acting along the flight path. The normal force equation balances lift and the vertical component of thrust against the component of weight. This equation ensures the aircraft does not rotate about the y-axis. It sums the aerodynamic moments caused by the wing and the elevator deflection. [5] These equations are then solved with a numerical solver to yield the trim condition state variables.

$$\mathrm{X} = T\cos\alpha - \frac{1}{2}\rho V^2 S\left(C_{D_{min}} + K\left(C_L - C_{L_{min}}\right)^2\right) - W\sin\theta = 0$$

$$\mathrm{Y} = \frac{1}{2}\rho V^2 S\left(C_{L_0} + C_{L_\alpha}\alpha + C_{L_{\delta_e}}\delta_e\right) + T\sin\alpha - W\cos\theta = 0$$

$$\mathrm{M} = \frac{1}{2}\rho S\bar{c}\left(C_{m_0} + C_{m_\alpha}\alpha + C_{m_{\delta_e}}\delta_e\right) = 0$$

The lateral-directional trim condition (steady coordinated turn) is a complex trim condition where the aircraft maintains a constant turn rate (psi_Dot) at constant altitude and a sideslip angle of 0deg. [6]

In order to numerically solve for this trim condition, the non-linear equations for sideforce, rolling moment, and yawing momoment must be solved to find the required bank angle and control deflections that provide the centripedal force required for the steady coordinated turn manoevre.

A1.2: Stability & Canard Trim

A. Longitudinal static and manoevre stability

An aircraft’s tendency to return to its trimmed flight condition without pilot intervention after a pitch distrubance is called longitudinal static stability. For a system to be statically stable it must generate a restoring moment that opposes the disturbance and the gradient of the pitching moment coefficient (C_m with respect to the angle of attack (alpha) must be negative:

$$\frac{dC_m}{d\alpha} < 0$$

The more negative this gradient, the stronger the restoring moment and the more longitudinally stable the aircraft will be. [7]

In a standard configuration with a tailplane located at the aft of the aircraft, the CG is located behind the wing's aerodynamic center. During a pitch up disturbance, angle of attack on the wing increases which increases its lift and causing a positive pitching moment, destabilizing the aircraft. The tailplane's lift also increases, causing a restoring moment that overpowers the wing's moment, returning the aircraft to its trim condition and satisfying the stability condition $\frac{dC_m}{d\alpha} < 0$.

The Beechcraft Starship has a canard confirguration where, unlike a standard aircraft, the CG is located behind the canard and ahead the main wing's aerodynamic center. When angle of attack is increased during a pitch disturbance, the angle of attack of the canard increases, increasing its lift and causing a destabilizing positive moment. The angle of attack on the main wing also increases, increasing its lift. This this creates the restoring moment and ensures longitudinal static stability. [8] [9]

The main difference is in the canard configuration, the main wing ensures the longitudinal stability, not the control surface like in a standard configuration.

Maneouvre stability is a tendency for an aircraft to exhibit a steady normal acceleration in response to a pitch control input away from trim. Its defined by the aircraft's response to a change in Load Factor. A higher manoeuvre stability means a higher stick force is required per g of accelration. [10]

For a standard configuration, to achieve a pitch up manoeuvre, a positive pitching moment about the CG is required which is generated by an upward elevator deflection which decreases the angle of attack and lift of the elevator. This decreases the overall lift of the aircraft.
For a canard configuration, to achieve a pitch up manoeurvre, a positive pitching moment about the CG is required which is generated by a downward canard deflection which increase the angle of attack and lift of the canard. This increases the overall lift of the aircraft. The canards are also designed to stall before the main wing to prevent deep stall. [11]

Standard aircraft are more stable because the tail is a stabilizing surface that naturally resists rotation, forcing the pilot to overcome a strong restoring tendency in order to manoevre. In contrast, a canard is a destabilizing surface ahead of the center of gravity that naturally tends to increase the pitch angle, meaning the aerodynamics actively assist the manoeuvre rather than resisting it, resulting in lower inherent stability.

B. Derivation for trimming a canard aircraft [12]:

Total pitching moments about cg: $M = M_0 - L_w(h_0 - h)\bar{\bar{c}} + M_c + L_c x_c$
Assuming the canard aerofoil is symmetric: $M_c = 0$
The equation can be rewritten in terms of coefficients: $C_m = C_{m0} - C_{Lw}(h_0 - h) + C_{Lc}\bar{V}_c$
The coefficient of lift of the canard can be found: $C_{Lc} = a_0 + a_{1c}\alpha_c + a_{1c}\lambda + a_{2c}\delta$
Where a_0= 0 since assumed symmetric, a_{1f} is canard lift curve slope, λ and δ are canard sweep angle and canard elevator deflection respectively, and a_{2f} is canard elevator lift curve slope.
It is assumed that $\alpha_f = \alpha_w + i_f$, where i_f is the canard setting angle relative to the wing, neglecting downwash due to the large cross sectional area difference.
$\alpha_w = \frac{C_{Lw}}{a_w} \therefore C_{Lf} = a_{1f}\left(\frac{C_{Lw}}{a_w} + i_f\right) + a_{1f}\lambda + a_{2f}\delta$
Plug C_{Lf} back into C_m: $C_m = C_{m0} - C_{Lw}(h_0 - h) + \bar{V}_f\left[a_{1f}\left(\frac{C_{Lw}}{a_w} + i_f\right) + a_{1f}\lambda + a_{2f}\delta\right]$
For trim equilibrium $C_m = 0$, hence, for a given canard sweep angle λ:

$$\delta_{trim} = -\frac{1}{\bar{V}_f a_{2f}}\left(C_{m0} + \bar{V}_f a_{1f}(i_f + \lambda) + C_{Lw}\left[\bar{V}_f\frac{a_{1f}}{a_w} - (h_0 - h)\right]\right)$$

C. Flight test demonstration of longitudinal static stability [13]

The controls fixed static margin for a canard configuration is the term denoted in the square brackets above. This can be used in conjuction with flight test data to determine the longitudinal static stability.

1. Trim the aircraft for level flight at an arbitrary speed
2. Without re-trimming, pull the stick back and hold at various different speeds

3. Measure the control surface deflection (δ) required to maintain level flight at each speed and plot δ vs. C_L since C_L is proportional to $\frac{1}{V^2}$
4. Analyze the gradient if this plot. Since it is proportional to H_n, if the gradient is less than 0, $H_n > 0$, so aircraft is stable. If the is gradient > 0, aircraft is unstable and if = 0, the aircraft is at the neutral point.

A2.1: Aerodynamic Coupling for an Oblique Wing

The AD-1, particularly at a high wing sweep angle of 60deg, loses longitudinal symmetry. This results in inherent aerodynamic and inertial cross-coupling between the longitudinal (pitch) and lateral-directional (roll, yaw, sideforce) axes. To analyze this, the aircraft is assumed to be a rigid body where the sum of all forces and moments must equal zero for trimmed flight. Because the OWRA and AD-1 utilize the same oblique wing platform, their coupled dynamic behavior is treated as identical for this analysis. [14]

Asymmetric Coupling Mechanisms

In a standard symmetric aircraft, longitudinal forces do not create lateral moments because the aircraft geometry is a mirror image across the X-Z plane. [15] The oblique wing breaks this symmetry so the swept wings generate differential lift and sideforce which induce major cross-coupling effect.

- Pitch-to-Roll Coupling (L_alpha): As Angle of Attack (alpha) increases, the lift distribution becomes asymmetrical relative to the center of gravity. The forward-swept wing experiences different local flow conditions compared to the aft-swept wing. [16] This lateral imbalance of lift forces creates a net rolling moment (L) purely as a function of pitch input (alpha). $L_\alpha = \partial L/\partial \alpha \neq 0$
- Pitch-to-Sideforce Coupling (Y_alpha) caused by Leading-Edge Suction: On a standard wing, left and right suction vectors cancel each other out. On an oblique wing, the leading edge is a continuous diagonal line, meaning the lateral components of the suction vectors all point in the same direction. As alpha (and lift) increases, these vectors sum to create a large net sideforce (Y) that pushes the aircraft sideways. [17]

Control Surface Usage for Asymmetric Trim

To quantify the control forces required to balance these coupled effects, we use Strip Theory. This models the total aerodynamic force as the integral sum of forces generated by individual 2D airfoil sections ("strips") of width dy along the span. [18]

1. **Aileron** (ξ): The ailerons are the primary surface for generating corrective rolling moment (L_ ξ) to counter the pitch-to-roll coupling to ensure trimmed flight. However, due to the differential forces acting on the swept platform, they also generate significant cross-coupling in pitch and yaw. [19]
    - Rolling Moment (L_ξ) - Primary: Derived by integrating the differential lift moment (Lift x lateral arm y) across the aileron span (y_1 to y_2).
    $$L_\xi = (\partial L)/(\partial \xi) = -1/2\, \rho V^2 a_{(2A)} \int (y_1)^{(y_2)} c_y\, y\, dy$$
    - Coupled Yawing Moment (Nξ): Aileron deflection generates differential drag. This drag force acting at lateral arm y is integrated to find the yawing moment.
    $$N_\xi = (\partial N)/(\partial \xi) = 1/2 \rho V^2 \int (y_1)^{(y_2)} \left((\partial C_{(Dy)})/(\partial \xi)\right) c_y\, y\, dy$$
    - Coupled Pitching Moment (Mξ) Because the wing is swept, the strip at spanwise position y is displaced longitudinally by a distance x(y) relative to the Center of Gravity. The differential lift acting at this longitudinal arm creates a pitching moment.
    $$M_\xi = -\frac{1}{2}\rho V^2 \int_{y_1}^{y_2} \left(\frac{\partial C_L}{\partial \xi}\right) c(y)\, x(y)\, dy$$
2. **Elevator** (eta): The elevator provides the primary pitching moment (M_eta). Due to the asymmetric wake from the oblique wing, symmetric elevator input creates minor coupled rolling (L_eta) and yawing (N_eta) moments.
    - Pitching Moment (M_eta): Calculated by integrating the tail lift slope across the elevator span, acting at the local longitudinal tail arm x_t(y).
    $$M_\eta = \frac{\partial M}{\partial \eta} = -\frac{1}{2}\rho V^2 \int_{y_{e1}}^{y_{e2}} \left(\frac{\partial C_{Lt}}{\partial \eta}\right) c_t(y)\, x_t(y)\, dy$$
3. **Rudder** (zeta): The rudder neutralizes yawing moments and the large aerodynamic sideforce (Y_alpha). It is integrated vertically along the fin span (z).

- Yawing Moment (N_zeta): Derived by integrating the side-force generated by the rudder acting at the longitudinal arm x_r(z).
$$N_\zeta = \frac{\partial N}{\partial \zeta} = -\frac{1}{2}\rho V^2 a_{2R} \int_{z_{r1}}^{z_{r2}} c_r(z)\ x_r(z)\, dz$$
- Sideforce (Y_zeta) - Primary Force: Unlike conventional aircraft where sideforce is negligible, the AD-1 requires significant sideforce to be generated to oppose the wing's suction coupling (Y_alpha). This is the integral of the lift generated by the vertical fin strips:
$$Y_\zeta = \frac{1}{2}\rho V^2 a_{2R} \int_{z_{r1}}^{z_{r2}} c_r(z)\ dz$$

Trim Balance Equations:

The final trim state is a highly coupled system of equations. The pilot must deflect ξ,η,ζ so that the control moments and forces oppose the inherent stability forces and moments (Fixed and alpha) and the cross-coupling cuased by the other controls.

$$L_\xi \xi + L_\eta \eta + L_\zeta \zeta + L_\alpha \alpha + L_\beta \beta + L_{\text{fixed}} = 0$$
$$M_\eta \eta + M_\xi \xi + M_\zeta \zeta + M_\alpha \alpha + M_{\text{fixed}} = 0$$
$$N_\zeta \zeta + N_\xi \xi + N_\eta \eta + N_\alpha \alpha + N_\beta \beta + N_{\text{fixed}} = 0$$
$$Y_{\text{total}} = Y_\alpha \alpha + Y_\zeta \zeta + Y_\xi \xi + Y_\beta \beta + Y_{\text{fixed}} + W \sin\phi \cos\theta \approx 0$$
$$Z_{\text{total}} = Z_\alpha \alpha + Z_\eta \eta + Z_\xi \xi + Z_\zeta \zeta + Z_{\text{fixed}} + W \cos\phi \cos\theta \approx 0$$
$$X_{\text{total}} = X_{\text{Thrust}} + X_\alpha \alpha + X_\beta \beta + X_{\text{drag\_controls}} + X_{\text{fixed}} + W \sin\theta \approx 0$$

Definition of "Fixed" Terms: These represent the residual aerodynamic moments present when alpha, beta, and all control deflections are zero. In the AD-1, these are non-zero due to the geometric asymmetry of the wing's thickness and camber relative to the airflow, as well as any built-in incidence or twist. [20]

A2.2: Stability Modes and Handling Qualities

The AD-1 fundamentally breaks the assumption of symmetry required for the five classical modes of motion to remain decoupled. In conventional aircraft, these modes are categorized into longitudinal (symmetric) and lateral-directional (asymmetric) sets. However, at sweep angles up to 60deg, the AD-1's modes mix, causing severe deviations from conventional norms and degrading handling qualities as measured by the Cooper-Harper (CH) rating scale. [21]

Longitudinal Mode Coupling

The longitudinal modes, typically governing pitch and speed, become sources of severe lateral-directional transients in the AD-1. [22]

The short period mode is a well-damped oscillation in pitch rate (q) and angle of attack (alpha). In the AD-1, the SP mode couples strongly into the lateral-directional axes. The roll rate component (p) in the SP eigenvector can be more than twice the pitch component (q).

- Driven by the large cross-coupling derivatives, the pitch-to-roll coupling (L_alpha) causes significant rolling acceleration. In one open-loop case at 65deg sweep, a 3.9deg change in alpha caused a 360deg roll. Pitch-to-sideforce coupling (Y_alpha) generates high lateral acceleration (a_y) during pitch maneuvers. [23]
- This coupling leads to unacceptable CH ratings (Level 3) at high dynamic pressure, with pilots avoiding aggressive pitch inputs due to objectionable responses. [24]

The Phugoid mode is a low-frequency mode that generally remained stable and fixed throughout the flight envelope for the AD-1. Because its frequency is much lower than other modes, its impact on piloting was less demanding, though the poor damping led to slightly increased workloads. [25]

Lateral-Directional Mode Coupling

These modes usually didn’t result in major pitch changes but, due to being constantly influenced by the oblique wing's asymmetry and low directional stability, they exhibited major amounts of coupling. [26]

- Roll Subsidence: The time constant (T_r) decreased significantly with increasing sweep because roll damping (C_lp) and roll moment of inertia (I_x) reduce concurrently. Despite reduced control authority, the roll mode generally meets Level 1 requirements. [27]
- Spiral Mode: The AD-1 exhibited slight spiral instability driven by the effective dihedral derivative (C_lbeta) and roll-due-to-yaw derivative (C_lr). However, because the time constant was very large, it approaches neutral stability and achieves Level 1 flying qualities. [28]
- Dutch Roll: The AD-1 suffered from low directional stability (C_nbeta) which resulted in the pilot feeling a "jerky" or "ratchety" oscillation with pitch coupling. The damping ratio was often too low, failing to meet Level 1 requirements and resulting in Level 2 qualities where the aircraft would "wander" or "search" directionally. [29]

Cooper-Harper Ratings and Deficiencies
The unaugmented AD-1 was inherently unsuitable for mission tasks due to severe coupling. Pilot ratings deteriorated with increasing wing skew and dynamic pressure. [30]

- Best Case (Lambda=45deg): Maneuvers were satisfactory (CH 2-3, Level 1) despite minor coupling.
- Worst Case (Lambda=65): Precision maneuvers were objectionable (CH 5-7, Level 2/3).
- Critical Failure: The most troublesome characteristic was the residual side acceleration (a_y). The lateral acceleration parameter A(y/n) reached 0.332 in the worst condition, far exceeding the acceptable Level 1 limit of 0.05.

A2.3: Feedback Control Architecture for Decoupling

I. The Concept of Feedback and Control Augmentation

Feedback control is a fundamental part modern flight dynamics where the system's output is measured, compared against a command, and feed back to adjust inputs automatically. In the context of the AD-1, feedback control is used to "augment" the stability of the aircraft, creating a closed-loop system that compensates for the aircraft's natural deficiencies. [31]

The AD-1 displays significant cross-coupling not present in symmetric airplanes, specifically Pitch-to-Roll (L_alpha) and Pitch-to-Sideforce (Y_alpha) coupling. The primary objective of the Flight Control System (FCS) design was to obtain Stability Augmentation System that could achieve decoupling among the pitch, roll, and yaw axes, stabilizing the highly coupled and lightly damped motion of the vehicle. [32]

II. Control Design Architectures To implement control on such a complex system, two main control architecture methods are available:

- Decoupling (MIMO) Focus: Use a Multi-Input Multi-Output architecture to actively remove coupling effects. For example, the system moves the ailerons and rudder automatically to prevent roll during a pitch command likeImplicit Model Following (IMF) system where the "plant" (the actual aircraft) is forced to track the response of an idealized "model" that doesn't exhibit the coupling response. [33]
- Direct Control (SISO) Focus: These methodologies apply Single-Input Single-Output techniques to shape individual modes or control surfaces. Examples include Modal control, where each mode is solved for stability independently. [34]

III. Implementation of Implicit Model Following (IMF)

The specific goal of the IMF controller for the AD-1 was to force the asymmetric, difficult-to-fly Plant to behave exactly like an Ideal F-8 Model that handles perfectly. The architecture below is based off Morris' research and consists of five distinct components: [35]

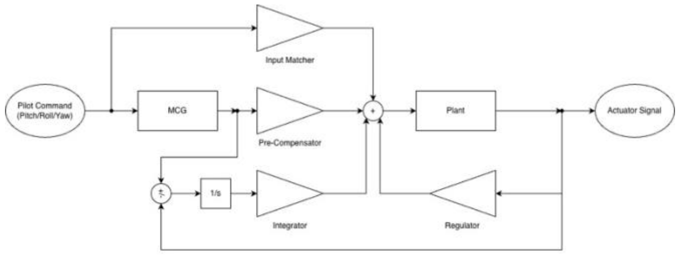

Figure 1, Control Architecture for IMF controller

Maneuver Command Generator (MCG): The MCG acts as the feedforward component. It is designed to have a perfect flying qualities and dynamic respons. It generates the target trajectory which dictates the desired modal decoupling such as specifying that a pitch command should result in zero roll.

Feedforward Control Logic: This logic functions as the translation layer between the MCG and the plant. It consists of an Input Matcher, which scales the pilot's inputs to the plant's sensitivity, and a State Pre-compensator. The Pre-compensator calculates the surface deflections required to achieve the MCG's trajectory by inverting the plant's dynamics. It applies immediate aileron and rudder inputs to cancel natural cross-coupling, effectively "hiding" the physical limitations of the oblique wing from the pilot.

Regulator (Full State Feedback): The Regulator is the core feedback element providing stabilization and disturbance rejection. It compares the actual states of the aircraft against the ideal states from the model. If the oblique wing begins to deviate, for example, rolling due to asymmetry, the regulator detects this error and applies opposing control inputs to enforce model tracking.

Integrator (Error Correction): The Integrator monitors the error between the MCG's output and the plant's actual output. If external factors like wind gusts or imperfections in the feedforward logic cause a deviation, the integrator accumulates this error and generates a progressively stronger corrective signal to drive the steady-state error to zero.

Linear Quadratic Regulator (LQR) Synthesis: The specific feedback and integral gains are calculated using LQR optimization. This technique involves a cost function that balances minimizing error and minimizing actuator effort. By assigning numerical weights, such as placing a heavy penalty on roll angle error, the optimal gains can be calculated.

During a manoeuvre, the systems follows the following steps:

1. The pilot applies a step input (pulls stick back).
2. The MCG simulates the perfect response (pure pitch-up with zero roll).
3. The Input Matcher instantly scales the pilot's stick input to match the plant's sensitivity while the Pre-compensator reads the MCG's changing states to anticipate dynamic needs. These two signals combine to send the exact mix of controls required to replicate the ideal response.
4. Sensors measure the actual motion of the AD-1 plant.
5. The Regulator compares this to the ideal state and applies correction if the aircraft deviates.
6. If a steady gap remains between the MCG and plant, the Integrator ramps up the control surfaces until the two trajectories overlap perfectly.
7. Signals from the Pre-compensator, Input Matcher, Regulator, and Integrator are summed to drive the control surfaces.

By implementing this Integrated Model-Following architecture, the deficiencies inherent to the AD-1, specifically its significant aerodynamic asymmetry and cross-coupling, are effectively hidden from the pilot. The feedforward logic essentially "inverse-models" the aircraft's physical limitations, instantly applying counter-inputs to neutralize the rolling moments that typically accompany high-g pitch maneuvers. Simultaneously, the high-gain regulator and integrator act as a safety net, actively suppressing any residual uncommanded motions or disturbances. This results in a system where the pilot experiences the crisp and decoupled responses of the Ideal Model rather than the sluggish and coupled dynamics of the physical airframe. This transforms a complex, difficult-to-fly research vehicle into a platform with Level 1 handling qualities.

A3.1: Flight Test Report: Performance and Stability

1. Executive Summary

This report documents flight tests conducted on a simulated Cirrus SR22 aircraft equipped with a Continental IO-550-N engine within the X-Plane 12 simulation environment. The primary objective was to validate evaluate the aerodynamic performance and dynamic stability characteristics and compare the simulation model against the certified Pilot's Operating Handbook (POH) and military flying qualities standards (MIL-F-8785C). All testing procedures and reporting adhere to NATO AGARDograph 300 Vol. 14 flight testing doctrine. [36] [37] [38]

2. Method of Test

Test Configuration: Testing was conducted in a Standard Atmosphere (ISA) with zero wind and turbulence and with the aircraft in a clean configuration (Flaps UP, Gear Fixed), and a total usable fuel capacity of 81 Gallons.

Data Acquisition:

- Performance: The aircraft was trimmed to steady level flight using autopilot atltitude hold at a constant 2500 ft. Subsequently, the throttle was carefully decreased to stabilise the aircraft at a range of different airspeeds from about 170 kts to stall to measure the power required.
- Stability: Specific control inputs were applied manually to excite dynamic modes. Results compared to Flight Phase Category B for a Class I aircraft.

3. Aerodyanmic Performance Results (Range and Endurance)

3.1.1 Physics-Based Fuel Flow Calculation Since the simulation data provided Power Required (HP), fuel consumption was calculated using specific engineering constants for the Continental IO-550-N engine. [39]

3.1.2 Theoretical Limits (No Reserves) Based on flight test data, the absolute aerodynamic limits (tank burned empty during constat altitude, no climb/descent) were identified using the governing equations for unaccelerated flight.

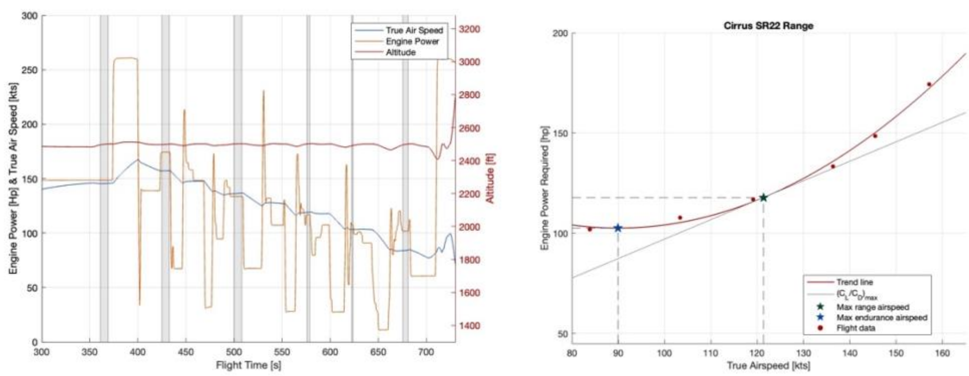

Figure 2, Left: Autopilot detected speed was approaching stall so turned off altitude stabilizer (that's why number 78 slithly above POH stall 71). Pitch down to stop stall causing altitude loss. Increased power to climb back up Right: Power vs Speed. Minimum power required to maintain level flight (V_be) is the minimum point of graph. Maximum Lift-to-Drag Ratio speed (V_br) is the tanget of the curve that passes through the origin.

	Speed [KTAS]	Power [HP]	Fuel Flow [GPH]	Theretical Max
Endurance	89.96	102.58	6.867	11.6 Hours
Range	121.35	117.83	7.855	1251 NM

3.1.3 Operational Cruise Performance (55% Power): Performance was evaluated against the POH at 55% Power (170 HP) with deductions for ground operations (-1.5 gal) and IFR reserves (-8.6 gal) so total fuel of 70.9 Gallons.

Comparison Table:

Parameter	Simulation Flight Test	Official Flight Manual (POH)*	Delta	%
Altitude	~2,500 ft	2,000 ft	+500	+20%
Cruise Speed [KTAS]	155.98	152	+3.98	+2.6%
Fuel Flow [GPH]	11.33	11.3	+0.03	+0.2%
Endurance [Hours]	6.26 Hours	6.2 Hours	+0.06	+1.0%
Range [NM]	976 NM	941 NM	+35 NM	+3.7%

- *POH Reference: Section 5, Page 5-31 (Range/Endurance Profile, 55% Power, Best Economy).

Discussion: The analysis highlights two key discrepancies between the simulation and the certified aircraft data:

- Aerodynamic Efficiency (Drag): The most significant finding is that the simulated aircraft is 4 knots faster (156 vs 152 KTAS) than the real aircraft at the same power setting and altitude. This suggests the simulation model represents a "clean" airframe that does not account for real-world parasite drag inducers found on the physical aircraft, such as antennas, gap seals, surface roughness, or paint condition.
- Range Benefit: Because of this speed advantage, the simulation yields an extra 35 Nautical Miles of range for the same fuel load. The fuel consumption rates are nearly identical, confirming that the simulated engine model is accurate, and the discrepancy is almost entirely aerodynamic.

4. Longitudinal Dynamic Stability

4.1.1 Short Period Mode Analysis

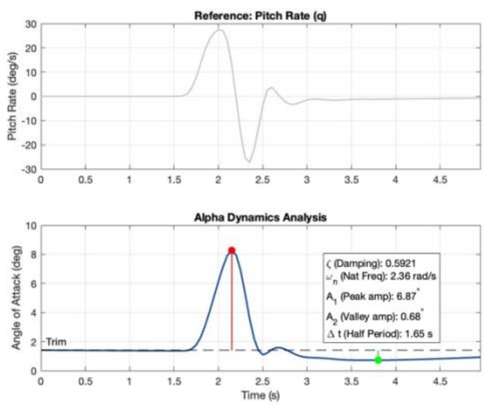

Figure 3, Short Period Response

- Theory: The Short Period Pitching Oscillation (SPPO) is a rapid, damped oscillation in pitch about the oy axis. It is characterized by rapid changes in pitch rate (q) and incidence (alpha), while forward speed (V) remains essentially constant.
- Test Method: The mode was excited by applying a short-duration (approx. 1 second) elevator pulse to the trimmed aircraft.
- Data Analysis: The pulse generated a sharp pitch rate response peaking at ~ 28deg/s, followed by rapid reversal and damping around a trim alpha of ~1.5deg.
- Measured Parameters:
  - Damping Ratio (zeta_sp): 0.5921
  - Undamped Natural Frequency (omega_sp): 2.36 rad/s
- Assessment:
  - Damping: Zeta_sp: 0.3 ≤ 0.5921 ≤ 2 so Level 1 Flying Handling
  - Control Anticipation (CAP): Referring to the "Thumb Print Criterion", a frequency of ~2.3 rad/s combined with a damping of ~0.6 places the aircraft in the "Satisfactory" zone.

4.1.2 Phugoid Mode Analysis

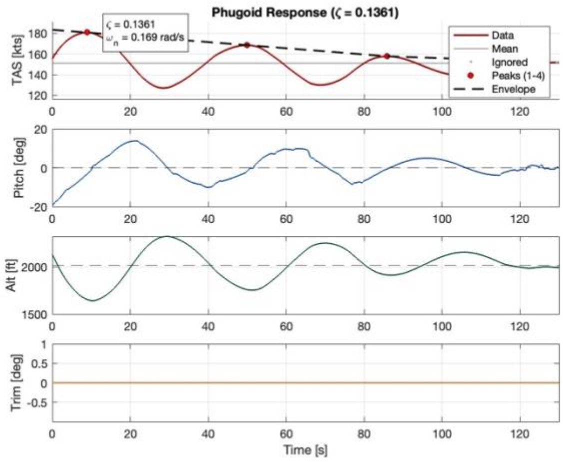

Figure 4, Phugoid Response

- Theory: The Phugoid is a lightly damped, low-frequency oscillation involving the exchange of kinetic energy (speed) and potential energy (height) while incidence (alpha) remains constant.
- Test Method: Excited by a "stick down" input to increase speed away from trim, then returning elevator to trim to allow oscillation.
- Data Analysis: True Airspeed (TAS) and Altitude traces exhibited the classic anti-phase (180deg shift) relationship.
- Measured Parameters:
  - Damping Ratio (zeta_p): 0.1361
  - Undamped Natural Frequency (omega_p): 0.169 rad/s
- Theoretical Validation of the phugoid mode (Lanchester Model):
  - Theoretical Frequency $\omega_p \approx \frac{g\sqrt{2}}{V_0}$.
  - With V_trim ~80 m/s (155 kts): $(9.81 \times 1.414) / 80 \approx 0.173$ rad/s.
  - Correlation: The measured 0.169 rad/s matches theory closely.
- Assessment:
  - Damping: Level 1 requires zeta_p > 0.04. The measured 0.136 exceeds this significantly.

4.1.3 Mode Coupling Check

- Requirement: It is desirable that $\omega_p/\omega_{sp} \leq 0.1$ to avoid handling difficulties.
- Result: $0.169/2.36 = \mathbf{0.07}$ The modes are effectively decoupled, ensuring that pilot inputs for maneuvering (Short Period) do not inadvertently excite the long-term speed oscillation (Phugoid).

5. Lateral-Directional Dynamic Stability

5.1.1 Dutch Roll Mode Analysis

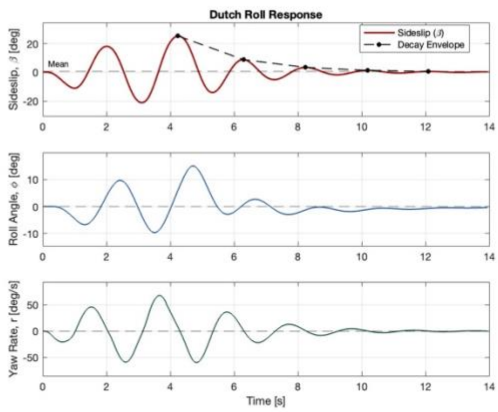

Figure 5, Dutch Roll Response

- Theory: A damped oscillation in yaw coupled into roll and sideslip.
- Test Method: Excited by a rapid cyclic rudder pedal input (doublet).
- Data Analysis: Clear oscillatory response observed. There is a noticeable phase lag between yaw rate and roll angle peaks (~ 90deg).
- Measured Parameters:
  - Period (T_d): 1.96 s
  - Damping Ratio (zeta_d): 0.1647
  - Natural Frequency (omega_d): 3.245 rad/s
- Assessment: Meets Level 1
  - Damping: Measured 0.1647 > Min 0.08. (Pass)
  - Frequency: Measured 3.245 > Min 0.4. (Pass)
  - Product (zeta_d \omega_d): $0.1647 \times 3.245 = \mathbf{0.534}$ > Min 0.15. (Pass)

5.3.2 Roll Subsidence Mode Analysis

- Theory: A non-oscillatory, exponential decay of rolling motion governed by damping in roll (L_p). When an aircraft is rolling and the ailerons are neutralized, the roll rate (p) should decay to zero exponentially. This mode determines how "crisp" the aircraft feels in roll.
- Test Method: Aircraft established in a bank, then ailerons abruptly neutralized.
- Assessment:
    - Requirement: Level 1 requires $T_r \leq 1.0$ s.
    - Result: 0.11 s is significantly less than 1.0 s.
    - Implication: The aircraft stops rolling almost instantaneously when the stick is centered, indicating "crisp" handling.

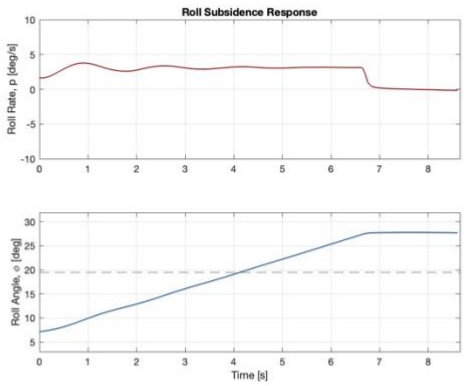

Figure 6, Roll Subsidence Response

5.3.3 Spiral Mode Analysis

- Theory: Non-oscillatory mode determined by the balance of directional and lateral static stability. A stable spiral mode returns wing to level after a bank, and unstable mode causes the aircraft to slowly diverge in roll and yaw, entering a tightening spiral dive if unchecked.
- Test Method: Aircraft established in a steady 28° banked turn, controls released.
- Data Analysis: Roll angle slowly diverged from 28° to 68° over 26 seconds. Confirmed Unstable.
- Measured Parameters:
    - Time Constant (T_s): 30.30 s
    - Time to Double Amplitude (T_2): 21.00 s

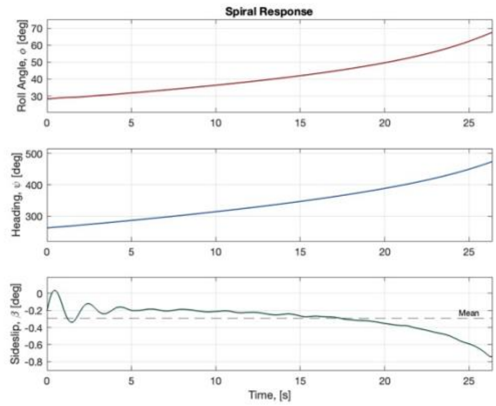

Figure 7, Spiral Mode Response

- Assessment:
    - Requirement 1: Level 1 requires T_2 > 20 s. (Measured 21.00 > 20.0).
    - Requirement 2: Level 1 requires T_s > 28.9 s. (Measured 30.30 > 28.9).
    - Conclusion: Although unstable, the divergence is slow enough to meet Level 1 limits, presenting minimal pilot workload.

6. Conclusions

    - Performance: The simulation predicts a practical cruise range of 976 NM, which aligns closely to the POH
    - Dynamic Stability: The flight test program confirms that the Cirrus SR22 simulation model exhibits Level 1 Flying Qualities across all tested longitudinal and lateral-directional modes.

B1.1: System Identification and Transfer Function

The transfer function was derived assuming a second-order system approximation. The pitch response data was analyzed to determine steady-state values and transient characteristics. [40]

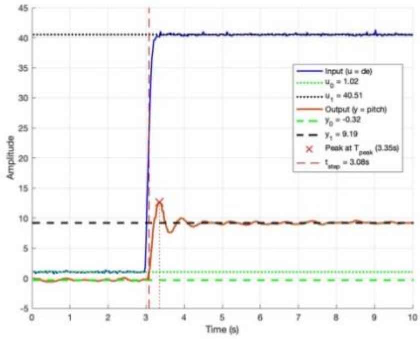

Figure 8, Experimental Pitch Reponse

The time at which the pitch change starts in defined as T_{step}. The average deflection (u_0) and pitch before the step are defined as (u_0) and (y_0) respectively. The steady state deflection (u1) and pitch after the step are defined as (u1) and (y1) respectively.

T_{step}	u0	y0	u1	y1	y_peak	T_peak
3.0761	1.02	-0.325	40.507	9.1854	12.6195	3.3508

The Steady-State Gain (K), Time to Peak (Tp), and Percent Overshoot (P.O) were found using the following equations:

$$K = \frac{y1 - y0}{u1 - u0} = 0.2408, Tp = Tpeak - Tstep = 0.27467, P.O. = \frac{ypeak - y1}{y1 - y0} = 36.1\%$$

The Damping ratio (ζ) and Natural Frequency (ω_n) can be found by rearraniging Dorf's equations:

$$\zeta = \sqrt{\frac{(-\ln P.O.)^2}{\pi^2 + (\ln P.O.)^2}} = 0.3084,$$

$$\omega_n = \frac{\pi}{Tp\sqrt{1 - \zeta^2}} = 12.024$$

Finally, the transfer function and be calculated:

$$G(s) = \frac{K\omega_n{}^2}{s^2 + 2\zeta\omega_n s + \omega_n{}^2} = \frac{34.8215}{s^2 + 7.4173s + 144.5778}$$

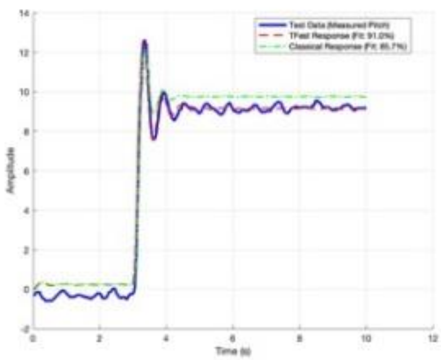

Figure 9, Comparison of Step reponses

To validate this result, the MATLAB `tfest` function was used to estimate the transfer function iteratively. The `tfest` model provided a closer fit to the experimental data than the classical calculation, capturing the system dynamics more accurately but the classical calculation transfer function was used in the follow question. Tfest extra zero. Note that the classical TF was designed to match the peak response, not the steady state which is why it results in a slight steady state error.

B1.2: Controller Design (Frequency Domain)

The goal is to design a PI or PID pitch controller for the plant G(s) defined in B1.1 to track a reference input and stabilize against disturbances. [41, 42] The following minimum performance specifications were defined:

1. Crossover Frequency (ω_c): The crossover frequency is a primary specification for the speed of response (or bandwidth). A ω_c of 10 rad/s ensures a fast-reacting system. [43]
2. Phase Margin (PM): The phase margin specification dictates the stability and transient response (overshoot). [44]

- A PM = 45° target represents an "Aggressive" design. It meets the bare minimum of the specification and corresponds to a damping ratio of ~0.45, which will result in a fast response but a significant theoretical percent overshoot (P.O.) of around 20%.
- A PM = 60° target represents a "Robust" design. This is a common, safer target that provides a larger stability margin. It corresponds to damping ratio of ~0.6 and a much smaller P.O. of around 10%.

First, the uncompensated plant is analyzed. At ω_c = 10 rad/s, the plant has:

- Magnitude: |G_p(ω_c)| = 0.4023
- Phase: ∠G_p(ω_c) = -59.0°

The PI controller G_c(s) = K_p + K_i/s is solved using the requirements:

K_p = |G_c| / sqrt(1 + tan(∠G_c)^2)

K_i = -ω_c * K_p * tan(∠G_c)

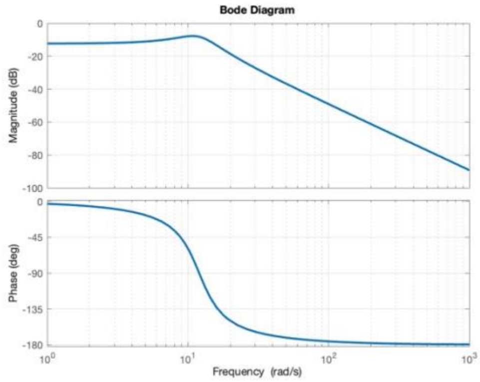

Figure 10, Bode plot of uncompensated system

- Required Controller Magnitude: |G_c| = 1 / |G_p(ω_c)|
- Required Controller Phase: ∠G_c = -180° + Target PM - ∠G_p(ω_c)

Design 1: "Aggressive" PI Controller (Target PM = 45°)

|G_c|	∠G_c	K_p	K_i
2.485	-76°	0.601	24.1

Design 2: "Robust" PI Controller (Target PM = 60°)

|G_c|	∠G_c	K_p	K_i
2.485	-61°	1.218	21.97

Design 3: "Optimal" PID (Pole-Zero Cancellation)

To eliminate the trade-off between speed and overshoot, a pole-zero cancellation method was applied. Instead of designing for a specific Phase Margin, the PID controller's two zeros were used to cancel the plant's two poles. [45]

- Plant Denominator = s^2 + 7.417s + 144.5778
- PID Numerator = Kd*s^2 + Kp*s + Ki

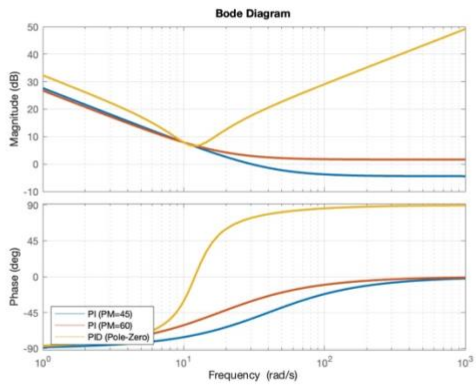

Figure 11, Bode plot of controllers

The PID numerator was set to be a multiple C of the plant denominator:

Kd*s^2 + Kp*s + Ki = C * (s^2 + 7.417s + 144.5778)

This results in a simplified open-loop transfer function:

L(s) = (C * 34.8215) / s

We solve for C to meet the bandwidth spec |L(ω_c)| = 1:

C = 10 / 34.8215 = 0.287

The gains can then be solved with this C value yielding:

- Kd = C * 1 = 0.287
- Kp = C * 7.417 = 2.13
- Ki = C * 144.5778 = 41.49

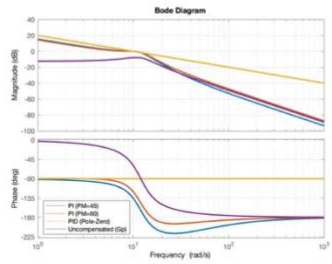

Figure 12, Bode plot of compensated system

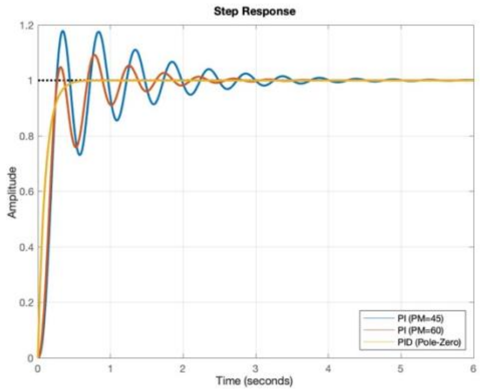

Figure 14, Step Reponse of Controllers

Figure 13, Controller disturbance rejection

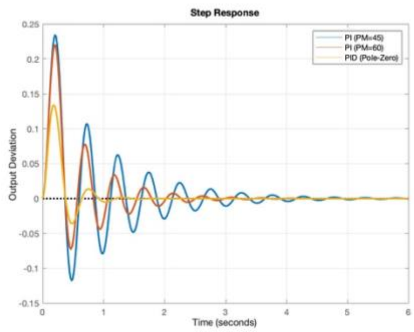

Controller	PM	Rise Time [s]	Overshoot Percentage [%]	Settling time [s]	Disturbance peak deviation	Disturbance Settling time [s]
PI	45	0.1595	17.89	2.911	0.2342	3.7841
PI	60	0.1677	9.2665	1.7916	0.2197	2.4027
PID	90	0.2197	0.0000	0.3912	0.1339	1.1145

Conclusion The "Aggressive" design is 5% faster but suffers from ~18% overshoot. The "Robust" design reduces overshoot by half in comparison (~9%) and settles 40% faster, making it the superior PI choice. The "Optimal" PID offers perfect performance (0% overshoot) but requires a derivative term (K_d), which may amplify noise in real-world applications. Also, if the real-world plant model differs even slightly from G_p(s), the pole-zero cancellation will fail, and the actual performance may degrade so the PI controllers will be more robust to model imperfections. [46]

B2.1: Root Locus and CG Variation

The root locus presented tracks the trajectory of the aircraft's longitudinal poles as the Center of Gravity (X_cg) varies. Difficulty extracting because model doesn't output mode correlation

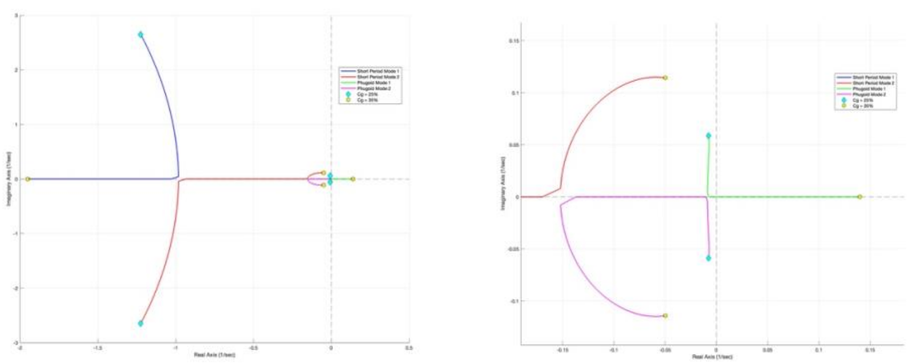

Figure 15, Root locus from 25% to 35% CG

As the CG moves aft (from the cyan diamonds at 25% to the yellow stars at 35%), the aerodynamic stability of the aircraft decreases significantly, leading to instability. [47]

1. Short Period Mode Analysis (Blue & Red Traces)

The Short Period mode is typically a fast, well-damped oscillation involving pitch rate (q) and angle of attack (alpha).

- Initial State (25% - Cyan Diamonds): The poles start as a complex conjugate pair far to the left (approx. real -1.2, imag 2.6). This indicates a stable, oscillatory mode with high natural frequency and good damping. The aircraft is statically stable here.
- Transition and Bifurcation: As x_cg moves aft, the static margin decreases.The complex poles migrate toward the real axis, representing a reduction in natural frequency and increase in damping. They eventually meet on the real axis (critical damping) before splitting
- Final State 30% (Yellow Stars): After meeting on the real axis, the poles split. One pole moves further left (becoming more stable/faster convergence). The other pole moves to the right, becoming less stable

2. Phugoid Mode Analysis (Green & Magenta Traces)

The Phugoid mode is a slow, lightly damped oscillation involving an exchange of kinetic energy (speed) and potential energy (altitude).

- Initial State (25% - Cyan Diamonds):
    - The poles are very close to the origin and the imaginary axis. This represents a long-period oscillation with very low damping (which is typical for the Phugoid mode).
    - The Split (Bifurcation): Once on the real axis, the poles split. One moves left (becoming a stable subsidence), and the other moves right (into the Right Half Plane).
    - The Unstable Root (Positive Real Pole): The yellow star at approx $+0.2$ represents the instability.
- Physical Meaning: This is a Non-Oscillatory Divergence. Because the aircraft is now statically unstable (CG aft of Neutral Point), a small disturbance in pitch will not self-correct. Instead, the aircraft will continue to pitch up and slow down (or pitch down and speed up) monotonically until it departs controlled flight. [42]

B2.2: PI Feedback Control Implementation

Architecture: PI Control with full state feedback

To stabilize the aircraft at the unstable center of gravity (x_cg = 35%), a feedback control system was implemented. While classical PI designs typically feed back only the error, this design utilizes full State Feedback. This is functionally a PI controller enhanced with additional state information for robustness creating a full Stability Augmentation System. [48]

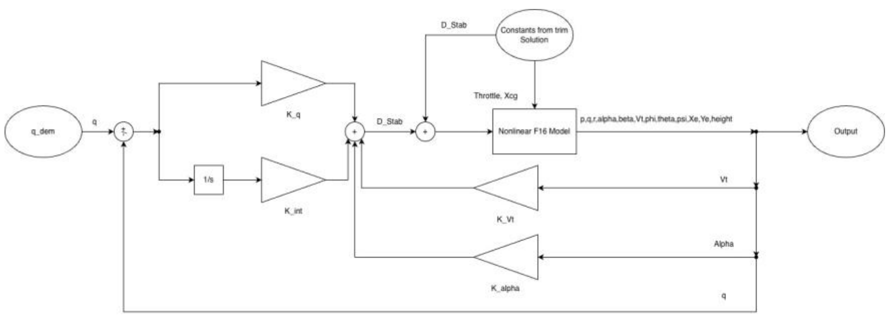

Figure 16, PI with full state Feedback architecture

- Proportional Term (q): The pitch rate state. Feedback on this term (K_q) acts as the Proportional gain, providing the necessary "stiffness" and artificial damping to stabilize the divergent mode.
- Integral Term (x_i): An augmented state representing the integral of the error ($\int(q_{dem} - q)dt$). Feedback on this term (K_{int}) ensures zero steady-state error.
- Auxiliary Terms (alpha, V_t): Feedback on angle of attack and velocity provides additional regularization, though the q and int terms dominate the response.

The gains were selected using LQR optimization. To achieve Cooper-Harper Level 1 handling qualities, an iterative tuning process was employed to select the weighting matrices Q and R. The objective was to map the closed-loop eigenvalues of the Short Period mode ($\omega_{n,sp}$, ζ_{sp}) directly into the "Satisfactory" regions of standard flight dynamics criteria (Cook and Kolk). [49] [50] [51]

The natural frequency of the closed-loop response is primarily driven by the balance between the allowable control effort (R) and the penalty on tracking error (Q_{int}).

- Initial Design (R=1.5): The initial design yielded a natural frequency of $\omega_n \sim 1.1$ rad/s. According to the Pilot Opinion Contours (Cook, Fig. 2), this falls into the "Acceptable" but sluggish region, insufficient for a fighter aircraft.
- Optimization (R=0.1): To increase agility, the control effort penalty was reduced to R=0.1. This effectively "cheapened" the use of the stabilator, allowing the controller to command faster rates.
- Result: This adjustment shifted the natural frequency to $\omega_n \sim 2.95$ rad/s. This value aligns perfectly with the center of the "Satisfactory" bullseye in Cook's criteria, ensuring the response is responsive without entering the "Abrupt" region (> 4 rad/s).

The damping ratio is controlled by the penalty on the pitch rate state (Q_q), which acts as artificial damping.

- Initial Design ($Q_q = 25$): This setting produced a critically damped "deadbeat" response ($\zeta \sim 0.9$). While stable, this region is characterized in the Pilot Attitude chart (Kolk, Fig. 4a) as "Heavy" or "Stiff," meaning the aircraft resists rotation too aggressively.
- Optimization ($Q_q = 10$): The pitch rate penalty was relaxed to $Q_q=10$ to reduce this stiffness.
- Result: This adjustment lowered the damping ratio to $\zeta \sim 0.86$. This places the system in the optimal region of the "Thumbprint" chart (Kolk, Fig. 4b). The response now exhibits a negligible but physically desirable overshoot (~5%), providing the pilot with immediate feedback that the aircraft is rotating freely, while still settling almost instantly.

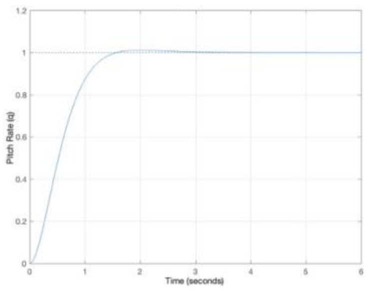

Figure 17, Step Reponse from LQR gains

As shown in the simulated step response, this configuration achieves the optimal compromise: it is fast enough to track agile targets (Level 1 Agility) but sufficiently damped to prevent pilot-induced oscillation (Level 1 Stability).

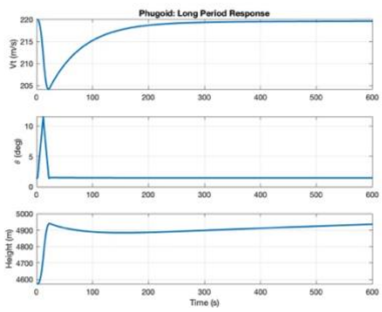

Figure 18, Phugoid reponse on non-linear system

To rigorously test the robustness of the designed controller, it was implemented within the full F-16 Non-Linear Simulation Model.

The system was subjected to a Pitch Rate Doublet command (q_{dem} = +/- 1deg/s for 10s each). This maneuver is a standard handling qualities test designed to excite both the short-period and phugoid modes of the aircraft.

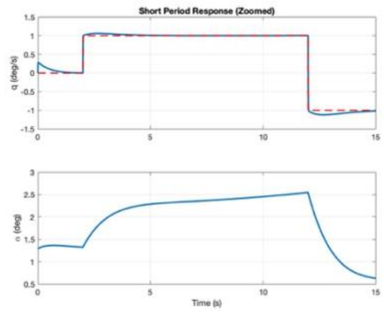

Figure 19, Short period reponse of non-linear model

Short Period (Agility): The response tracks the pilot command with minimal lag. The non-linear aerodynamics introduce a slight overshoot, but it settles within 2 seconds. The Angle of Attack evolves smoothly, peaking at approximately 2.5deg. There is no high-frequency chatter or instability in the alpha response, indicating the controller is effectively coordinating the turn.

Phugoid Suppression: In an unaugmented aircraft, this input would cause long-period oscillations. The controller successfully suppresses the Phugoid since velocity recovers monotonically after the altitude also stays stable and doesn't go unstable as the root locus plot

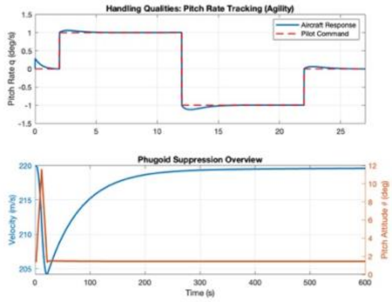

Figure 20, Handling comparison on non-linear model

The controller performance is acceptable and demonstrates Cooper-Harper Level 1 characteristics in the non-linear domain. The controller successfully stabilizes the 35%Cg unstable airframe throughout a dynamic maneuver, despite the non-linearities present in the simulation. The steady-state tracking error is effectively zero, validating the integral action design. The suppression of the phugoid mode and the predictability of the short-period response imply that the pilot would not need to constantly compensate for drift or oscillation, allowing them to focus on mission tasks.

B2.3: PI Feedback Control Implementation

B2.3: Low Speed Performance Analysis (V_t = 100 m/s)

The controller designed for 220 m/s was tested at a low-speed trim of V_t = 100 m/s.

- Aerodynamics: Dynamic pressure is ~20% of the design case, drastically reducing control surface effectiveness. Trim Angle of Attack (alpha) is high (~12deg) compared to the 1.4deg high-speed case. [52]

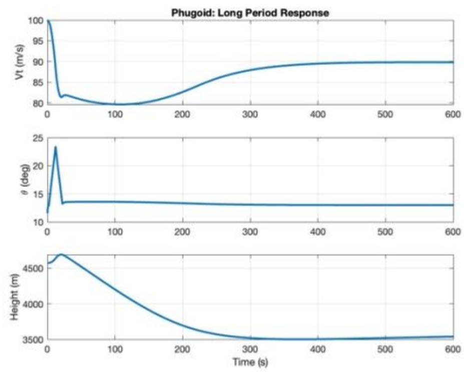

Figure 21, Phugoid reponse

Initialization Transient: As seen in the Handling Qualities plot, there is a massive transient spike in pitch rate at t=0 as the controller struggles to initialize at this off-design trim point.

Short Period (Agility): The low speed manoevre results in a bit more overshoot and longer settling time but overall the response is still acceptable. During the constant pitch rate command, the Angle of Attack (alpha) does not settle; it rises continuously from 12deg to over 16deg. This indicates the aircraft is struggling to generate the required turn rate without stalling or bleeding significant energy.

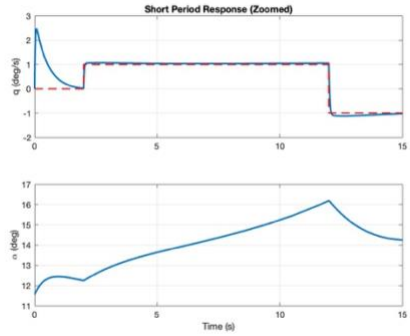

Figure 22, Short Period Reponse

Phugoid Suppression: The Phugoid Long Period plot reveals that the maneuver pushes the aircraft onto the back side of the power curve. [53] Velocity drops sharply from 100 m/s to a minimum of ~80 m/s before slowly settling at a new, lower equilib n level flight at this commanded pitch rate. The Height plot shows a continuous, linear descent, losing approximately 1100m (from 4600m to 3500m) over the 600-second simulation. The fixed-gain controller maintains pitch attitude but cannot compensate for the severe loss of energy.

Figure 23, Handling qualities comparison

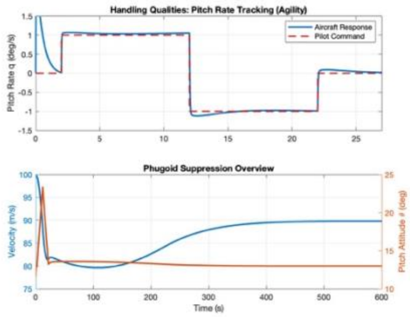

The primary limitation is that a linear controller designed for one operating point (220 m/s) is being applied to a vastly different aerodynamic condition (100 m/s). To improve overall effectiveness and robustness:

1. Gain Scheduling: This is the standard solution in flight control. Instead of fixed gains, the gains K should be functions of Dynamic Pressure (q_bar) or Velocity (Vt). As dynamic pressure decreases, the gains must generally increase to compensate for the reduced effectiveness of the control surfaces. [54]
    - K(q_bar) = K_design * (q_bar_design / q_bar_actual)
2. Alpha Limiter / Stall Protection: At 100 m/s, the trim alpha is already 12°. A pilot command could easily push the aircraft beyond the stall limit (approx. 25-30°). The controller should include a limiter that prevents the pitch demand from exceeding critical alpha. [55]
3. Auto-Throttle Integration: The severe altitude loss indicates that pitch control alone is insufficient at low speeds. An auto-throttle loop should be added to maintain velocity (Vt) by increasing thrust when the aircraft pitches up or enters a high-drag state.

B3.1: Comparison of Rate Limited Responses

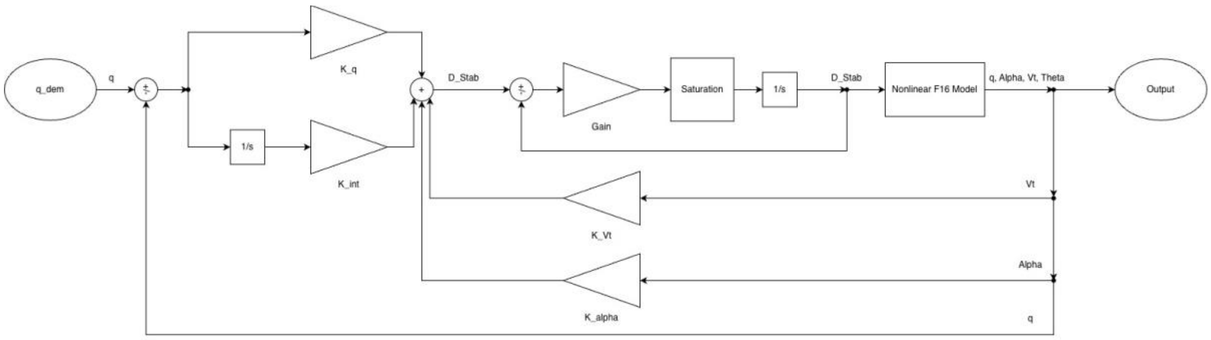

Figure 24, PI with Full state feedback on linear system with saturation

The simulation compares the response to a 5deg step demand of the linearized system under three actuator rate limit conditions. The results highlight the non-linear degradation of performance: [56]

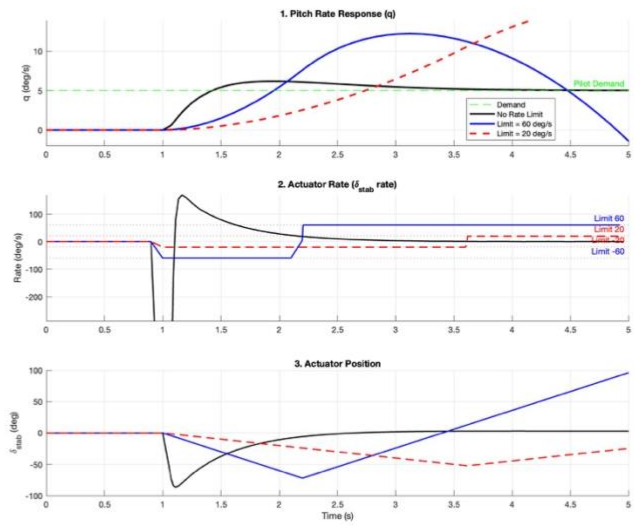

Figure 25, Response of linear system to 5deg/s q step

- No Rate Limit: The system exhibits the ideal linear response with a fast rise time and stable settling. However, the actuator rate plot reveals this requires an infinite initial rate which is physically impossible.
- Limit = 60 deg/s: The actuator saturates immediately, forcing the stabilator to move at a constant linear rate. This introduces a significant time delay in the controller causing Integrator Wind-Up. Because the error

remains non-zero for longer, the integral term accumulates an excessive value. This causes the response to overshoot the target significantly, continuing to rise past 8deg/s even after the actuator reverses direction, leading to dangerous oscillation.
- Limit = 20 deg/s: The system is even more severely rate-limited. The actuator cannot move fast enough to generate the required pitching moment at all. The response effectively turns into a slow ramp, failing to track the dynamics of the pilot's command. The aircraft would be judged as having Level 3 (Unacceptable) handling qualities due to extreme sluggishness.

B3.2: Mitigation for Actuator Rate Limiting

If the physical limitations of the hydraulic actuators cannot be upgraded, the control system must be modified to handle the saturation effects. The two primary methods to reduce the impact of rate limiting are anti-windup integration and command prefiltering.

Anti-Windup Integration:

The most severe issue observed in the rate-limited response (B3.1) was the significant overshoot caused by Integrator Wind-Up. [57]

- In a standard PI controller, the integral term (K_i) accumulates value as long as there is an error. When the actuator hits its rate limit, it falls behind the commanded rate. This causes the error signal to remain large for a longer duration than the design anticipated. This causes the integrator to "winds up" to a massive value as this error compounds. Even when the aircraft finally reaches the target pitch rate, the integrator is still holding this large value and commanding the actuator to stay at the limit. The system has to then overshoot the target significantly to generate enough negative error to "unwind" the integrator.
- An Anti-Windup scheme modifies the integrator logic to detects when the actuator has saturated and stop the integral error from accumulating.
- By stopping the accumulation of error during the saturation phase, the controller does not compute the period where it was unable to respond. As soon as the pitch rate reaches the target, the error is zero, the proportional term drops and the integrator allows the actuator to reverse immediately which eliminates the overshoot.

Command Prefiltering

Instead of trying to fix the saturation after it happens, command prefiltering ensures the controller never demands a rate that the aircraft cannot physically deliver. [58] [59]

- A step input from the pilot demands an infinite rate of change in pitch rate in this case. The linear controller sees this instantaneous error and commands the maximum possible actuator rate immediately. Since the physical actuator acts as a bottleneck, the control loop is broken, leading to the non-linear behavior **described above.**
- A Low-Pass Filter or a software rate limiter is placed on the pilot's command signal before it enters the feedback loop.
- This processes the step input into a smoother ramp input. If the filter is tuned such that the slope of the ramp is slightly below the physical limit of the actuator, the actuator would be able to track the demand. This results in a response that is slightly slower initially but is smooth, predictable, and free of oscillation.

References

[1] M. V. Cook, Flight Dynamics Principles Section 3.1.

[2] S. &. Lewis, Section 1.3.

[3] M. V. Cook, Flight Dynamics Principles Section 4.1.4.

[4] M. V. Cook, Flight Dynamics Principles Section 3.3.

[5] Nelson, Flight Stability and Automatic Control Section 2.4.

[6] F. S. a. A. C. Nelson, Section 2.7.

[7] Nelson, Flight Stability and Automatic Control Section 2.3.

[8] S. B. Anderson, A Look at Handling Qualities of Canard Configurations, NASA, 1896.

[9] FAA, Teardown Evaluation of a Composite Carbon/Epoxy Beechcraft Starship Aft Wing.

[10] M. V. Cook, Flight Dynamics Principles Section 8.

[11] S. B. Anderson, A Look at Handling Qualities of Canard Configurations, NASA, 1986.

[12] M. V. Cook, Flight Dynamics Principles Section 3.6.

[13] Nelson, Flight Stability and Automatic Control Section 2.3.

[14] NASA, A Piloted Eva1 iation of an Oblique-Wing Research Aircraft Motion Simulation With Decouphg Control Laws.

[15] M. V. Cook, Flight Dynamics Principles Section 4.3.

[16] L. Qiu, Decoupling control law design for OWRA, Chinese Flight Test Establishment.

[17] NASA, Integrated Aerodynamic and control system design of Obliquid wing aircraft.pdf.

[18] M. V. Cook, Flight Dynamics Principles Section 13.

[19] S. J. Morris, INTEGRATED AERODYNAMIC AND CONTROL SYSTEM DESIGN OF OBLIQUE WING AIRCRAFT, NASA.

[20] R. A. Kennedy, Experimental Aerodynamic Characteristics of an Oblique Wing for the F-8 OWRA, NASA.

[21] G. E. Cooper, The Use of Pilot Rating in the Evaluation of Aircraft Handling Qualities.

[22] M. V. Cook, Flight Dynamics Principles Section 6.2.

[23] NASA, A Piloted Evaluiation of an Oblique-Wing Research Aircraft Motion Simulation With Decouphg Control Laws.

[24] NASA, Flight Characteristics of the AD-1.

[25] NASA, Output Model-Following Control Synthesis for an Oblique-Wing Aircraft.

[26] M. V. Cook, Flight Dynamics Principles Section 7.2.

[27] A. G. Sim, Flight Characteristics of the AD-1, NASA.

[28] NASA, Flight characteristics of the AD-1.

[29] NASA, Flight Characteristics of the AD-1.

[30] NASA, A Piloted Evaluiation of an Oblique-Wing Research Aircraft Motion Simulation With Decouphg Control Laws.

[31] M. V. Cook, Flight Dynamics Principles, 2007.

[32] J. H. Vincent, APPLICATION OF MODERN CONTROL DESIGN METHODOLOGY TO OBLIQUE WING RESEARCH AIRCRAFT, NASA.

[33] NASA, Integrated Aerodynamic and Control.

[34] NASA, Modal Control of an Oblique Wing Aircraft.

[35] NASA, Integrated aerodynamic control.

[36] R. H. Prather, Pilot's Operating Handbook for the Cirrus SR22, FAA, 2003.

[37] A. FORCE, MIL-81882.

[38] NATO, RTO AGARDograph 300 - Intro to Flight Testing.

[39] S. Aviation, 550 T.I. ENGINE FOR THE BEECHCRAFT BONANZA.

[40] R. C. Dorf, Modern Control Systems.

[41] R. C. Dorf, Modern Control Systems.
[42] B. Etkin, Dynamics of Flight.
[43] Ogata, Modern Control Engineering.
[44] Franklin, Feedback Control of Dynamic Systems.
[45] Rivera, Internal Model Control.
[46] K. J. Astrom, PID controllers, Instrument Society of America.
[47] M. V. Cook, Flight Dynamics Princicles.
[48] R. C. Dorf, Modern Control Systems.
[49] M. V. Cook, Flight Dynamics Principles.
[50] W. R. Kolk, Modern Flight Dynamics.
[51] DoD, MIL-F-8785C.
[52] Nelson, Flight Stability and Automatic Control.
[53] Cook, Flight Dynamics.
[54] S. Lewis, Aircraft control.
[55] B. R. Cobleigh, High-Angle-of-Attack Yawing Moment Asymmetry, NASA.
[56] S. a. Lewis, Aircraft control.
[57] K. J. Astrom, PID Controllers, Instrument Society of America.
[58] F. Powell, Feedback Control of Dynamic Systems.
[59] S. Srinivasan, Adaptive Reference shaping.

Appendix

A3.1

Fuel Flow Equation:

$$\text{Fuel Flow (GPH)} = \frac{\text{Horsepower (HP)} \times \text{BSFC}}{\text{Fuel Density}}$$

Constants:

- BSFC (Brake Specific Fuel Consumption): 0.40 lb/hp/hr
    - Source: Summit Aviation / Continental Aerospace Technologies IO-550-N Performance Brochure (Range 0.385–0.41).
- Fuel Density: 6.0 lb/gal
    - Source: Cirrus SR22 POH Section 6.

Endurance Equation:

$$\text{Endurance (hr)} = \frac{\text{Total Fuel (gal)}}{\text{Fuel Flow (GPH)}}$$

Range Equation:

$$\text{Range (NM)} = \text{True Airspeed (kts)} \times \text{Endurance (hr)}$$

To generate a valid comparison with the certified Flight Manual, the following deductions must be applied to the fuel capacity.

1. Ground Operations Deduction: -1.5 Gallons
   - Requirement: Deducted for engine start, run-up, and taxi.
   - Reference: POH Section 5, "Time, Fuel and Distance to Climb" Note, Page 5-25.
2. IFR Reserve Requirement: -8.6 Gallons
   - Requirement: 45 minutes of flight at cruise power.
   - Reference: POH Section 5, "Range / Endurance Profile" Note, Page 5-29.
3. Net Usable Cruise Fuel: 70.9 Gallons
   - (81.0 Total - 1.5 Taxi - 8.6 Reserve).

Calculations:

- Fuel Flow: $\frac{170.5 \times 0.40}{6.0} = 11.4 \text{ GPH}$
- Operational Endurance: $\frac{70.9 \text{ gal}}{11.4 \text{ GPH}} = 6.2 \text{ Hours}$
- Operational Range: $157 \text{ kts} \times 6.2 \text{ hr} = 977 \text{ Nautical Miles}$